Chapter 2
Radial Basis Functions

Abstract The traditional basis functions in numerical PDEs are mostly coordinate functions, such as polynomial and trigonometric functions, which are computationally expensive in dealing with high dimensional problems due to their dependency on geometric complexity. Alternatively, radial basis functions (RBFs) are constructed in terms of one-dimensional distance variable irrespective of dimensionality of problems and appear to have a clear edge over the traditional basis functions directly in terms of coordinates. In the first part of this chapter, we introduces classical RBFs, such as globally-supported RBFs (Polyharmonic splines, Multiquadratics, Gaussian, etc.), and recently developed RBFs, such as compactly-supported RBFs. Following this, several problem-dependent RBFs, such as fundamental solutions, general solutions, harmonic functions, and particular solutions, are presented. Based on the second Green identity, we propose the kernel RBF-creating strategy to construct the appropriate RBFs.

Keywords Globally-supported RBFs · Compactly-supported RBFs · Operator-dependent · Kernel RBFs

The functions expressed in the Euclidean distance variable are usually termed as the radial basis functions (RBFs) in literatures. This is due to the fact that all such RBFs are radially isotropic due to the rotational invariant, and have become de facto the conventional distance functions of the widest use today. However, there do exist some quite important anisotropic and inhomogeneous RBFs, for instance, the spherical RBFs in handling geodesic problems and the so-called time–space RBFs. It is obvious that all these so-called anisotropic RBFs are not radially isotropic.

In terms of PDE kernel solutions, we have distance functions using three kinds of distance variables underlying (1) rotational invariant, (2) translation invariant, and (3) a scalar product of two vectors with the ridge function. The traditional rotational invariant RBFs do not cover the latter two. In addition, there are many other distance variables in the area of neural network and machine learning.

W. Chen et al., *Recent Advances in Radial Basis Function Collocation Methods*, SpringerBriefs in Applied Sciences and Technology, DOI: 10.1007/978-3-642-39572-7_2,

In most literature, the term "RBF" is, however, often simply used indiscriminatingly for the rotational and translation invariants distance variables and functions. Thus, this book extends the definition of RBF to general distance functions.

This chapter begins with an introduction of traditional RBFs for multivariate data interpolation, such as globally-supported RBFs and compactly-supported RBFs. In addition, several problem-dependent RBFs, such as fundamental solutions, general solutions, harmonic functions, and particular solutions, are also presented for the use in the following chapters. In the end, we introduce the kernel RBF-creating strategy.

2.1 Traditional RBFs

2.1.1 Globally-Supported RBFs

RBFs are mostly multivariate functions, and their values depend only on the distance from the origin, so that $\phi(\mathbf{x}) = \phi(r) \in R$, $\mathbf{x} \in R^n$, $r \in R$; or alternatively on the distance from a point of a given set $\{\mathbf{x}_j\}$, and $\phi(\mathbf{x} - \mathbf{x}_j) = \phi(r_j) \in R$. Any function ϕ satisfying the property $\phi(\mathbf{x}) = \phi(||\mathbf{x}||_2)$ is a radial function. The norm $r_j = ||\mathbf{x} - \mathbf{x}_j||_2$ is usually the Euclidean distance. Certainly, the other distance functions [1] are also possible. Some commonly used globally-supported RBFs are shown in Table 2.1.

Our interest lies in the RBF interpolation of a continuous multivariate function, $f(\mathbf{x}), \mathbf{x} \in \Omega \subset R^n$, where Ω is a bounded domain. Given N interpolation function values $\{y_i\}_{i=1}^N \in R$ at data location $\{\mathbf{x}_i\}_{i=1}^N \in \Omega \subset R^n$, then $f(\mathbf{x})$ can be approximated by a linear combination of RBFs, namely,

$$f(\mathbf{x}) \approx \sum_{j=1}^{N} \alpha_j \phi\left(\left\|\mathbf{x} - \mathbf{x}_j\right\|_2\right), \mathbf{x} \in \Omega, \tag{2.1}$$

Table 2.1 Commonly used globally-supported RBFs

RBFs	$\phi(\mathbf{x})$	CPD order (m)
Polyharmonic spline	$\begin{cases} r^{2k-1}, k \in \mathbb{N} \\ r^{2k}\ln(r), k \in \mathbb{N} \end{cases}$	$[k/2]+1$
Thin plate splines (TPS)	$r^2\ln(r)$	2
MQ	$(r^2+c^2)^k, k>0, k \notin \mathbb{N}$	$[k]+1$
IMQ	$(r^2+c^2)^{-k}, k>0, k \notin \mathbb{N}$	0
Gaussian	$e^{-(r^2/c^2)}$	0

$[k]$ denotes the nearest integers less than or equal to k, and $\mathbb{N}$ the natural number, c a positive constant which is known as the shape parameter, and CPD denotes the m-order conditionally positive definite functions [2]

where $\{\alpha_j\}$ are the unknown coefficients to be determined. By the collocation method, we have

$$y_i = f(\mathbf{x}_i) = \sum_{j=1}^{N} \alpha_j \phi\left(\left\|\mathbf{x}_i - \mathbf{x}_j\right\|_2\right),\ i = 1, \cdots, N. \tag{2.2}$$

The above linear system of equations can be expressed in the following matrix form

$$\mathbf{A}\alpha = \mathbf{b}, \tag{2.3}$$

in which $\boldsymbol{\alpha} = (\alpha_1, \alpha_2, \ldots, \alpha_N)^T$ is an unknown coefficient vector to be determined, $\mathbf{b} = (y_1, y_2, \ldots, y_N)^T$ is the right-hand side vector, and the RBF interpolation matrix is given by

$$\mathbf{A} = [\Phi_{ij}] = [\phi(||\mathbf{x}_i - \mathbf{x}_j||_2)]_{1 \le i,j \le N}. \tag{2.4}$$

However, some RBFs are conditionally positive definite functions as listed in Table 2.1, such as MQ and TPS. Hence polynomials are augmented to Eq. (2.1) to guarantee that the resultant interpolation matrix is invertible. Such a formulation is expressed as follows

$$f(\mathbf{x}) = \sum_{j=1}^{N} \alpha_j \phi(||\mathbf{x} - \mathbf{x}_j||_2) + \sum_{i=1}^{M} \alpha_{N+i} p_i(\mathbf{x}), \tag{2.5}$$

with constraints

$$\sum_{j=1}^{N} \alpha_j p_i(\mathbf{x}_j) = 0,\ i = 1, 2, \cdots, M, \tag{2.6}$$

in which $p_i \in \Pi_{m-1}, i = 1, 2, \cdots, M$, where Π_m represents the polynomial space that all polynomials of total degree less than m in n variables, $M = \begin{pmatrix} N+m-1 \\ m-1 \end{pmatrix}$.

Then, Eqs. (2.5) and (2.6) yield a matrix system of $(M+N) \times (M+N)$

$$\begin{bmatrix} \mathbf{A} & P \\ P^T & \mathbf{0} \end{bmatrix} [\boldsymbol{\alpha}] = \begin{bmatrix} \mathbf{b} \\ \mathbf{0} \end{bmatrix}. \tag{2.7}$$

To illustrate the stability and efficiency of the RBF interpolation, without loss of generality, we consider the following test functions on the 2D unit square domain

$$f_1 = f_a + f_b, \tag{2.8}$$

$$f_2 = \sin\left(\frac{\pi x}{6}\right) \sin\left(\frac{7\pi x}{4}\right) \cos\left(\frac{3\pi y}{4}\right) \cos\left(\frac{5\pi y}{4}\right), \tag{2.9}$$

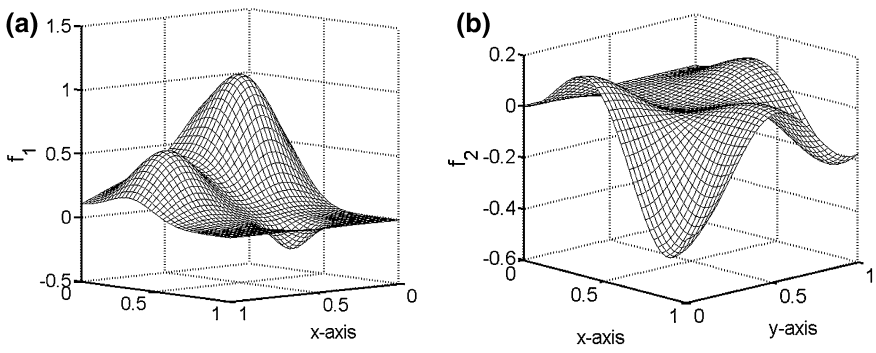

Fig. 2.1 Profiles of test functions **a** Eq. (2.8), **b** Eq. (2.9)

where

$$f_a = \frac{3}{4}\exp\left(\frac{-(9x-2)^2}{4} - \frac{(9y-2)^2}{4}\right) + \frac{3}{4}\exp\left(\frac{-(9x+1)^2}{49} - \frac{(9y+1)^2}{10}\right), \quad (2.10)$$

$$f_b = \frac{1}{2}\exp\left(\frac{-(9x-7)^2}{4} - \frac{(9y-3)^2}{4}\right) - \frac{1}{5}\exp\left(-(9x-4)^2 - (9y-7)^2\right). \quad (2.11)$$

Figure 2.1 shows the profiles of these two test functions. Note that f_1 is the well-known Franke's function [3]. We conduct numerical experiments via the MQ. This study defines the normalized root-mean-square error (Rerr) and the normalized maximum error (Mrerr) as

$$\text{Rerr} = \frac{1}{\max\limits_{1 \le i \le \text{NT}} |f_e(\mathbf{x}_i)|} \sqrt{\frac{1}{\text{NT}} \sum_{i=1}^{\text{NT}} |f(\mathbf{x}_i) - f_e(\mathbf{x}_i)|^2}, \quad (2.12)$$

$$\text{Mrerr} = \frac{1}{\max\limits_{1 \le i \le \text{NT}} |f_e(\mathbf{x}_i)|} \max_{1 \le i \le \text{NT}} |f(\mathbf{x}_i) - f_e(\mathbf{x}_i)|, \quad (2.13)$$

where $f_e(\mathbf{x}_i)$ and $f(\mathbf{x}_i)$ are the analytical and numerical solutions evaluated at $\mathbf{x}_i$, respectively, and $\text{NT} = 10,201$ is the total number of 101×101 uniformly distributed test points in a unit square domain.

In this study, we place the interpolation points with uniform spacing, h, for easy comparisons. From the numerical errors presented in Table 2.2, one can observe that

(a) The error decreases with the grid refinement.
(b) The condition number of RBF interpolation matrix increases with the grid refinement.
(c) The shape parameter c is very sensitive to the test functions and the grid size.

Table 2.2 Numerical errors using MQ RBF based on grid size $h = 0.1$ and $h = 0.05$

Functions	Grid size (h)	Optimal shape parameter (c)	Condition number	Mrerr	Rerr
f_1	0.1	0.16	3.4e + 05	1.2e−02	1.4e−03
f_1	0.05	0.31	3.8e + 14	2.8e−05	3.1e−06
f_2	0.1	1.16	3.2e + 17	8.5e−05	1.1e−05
f_2	0.05	0.78	6.6e + 19	3.4e−06	4.7e−07

Table 2.3 Error estimates of different RBFs with respect to grid size h

RBFs	$\phi(\mathbf{x})$	Error estimate
Polyharmonic spline	$\begin{cases} r^{2k-1}, k \in \mathbb{N} \\ r^{2k}\ln(r), k \in \mathbb{N} \end{cases}$	h^k
Thin plate splines (TPS)	$r^2\ln(r)$	h^2
MQ	$(r^2+c^2)^k, k>0, k \notin \mathbb{N}$	$e^{-a/h}$
IMQ	$(r^2+c^2)^{-k}, k>0, k \notin \mathbb{N}$	$e^{-a/h}$
Gaussian	$e^{-(r^2/c^2)}$	$e^{-a\ln h/h}$

(d) The accuracy in function f_1, with the grid size $h = 0.1$, is poor because the grid is too coarse to perform a more accurate solution.

From the above numerical experiments, we observe that the numerical accuracy depends on the grid size, the shape parameter, the complexity of the given functions, and the other potential factors. Great efforts have been made to find the relationship between the RBF interpolation's accuracy and that of various influential factors [4–8]. Duchon [9], Madych and Nelson [10–12], Wu and Schaback [13], and Cheng [14] made contributions to estimate the error of RBF interpolation. Wendland [15] made a summary of these estimates for different RBFs with respect to grid size h, which is presented in Table 2.3.

Theoretical analysis and empirical formulas for RBF interpolation are also proposed in literature but remain underdeveloped. Based on Madych's theoretical analysis [16], the error estimates of MQ, IMQ, and Gaussian RBFs are made up of the product of two rival terms. Namely, one part grows exponentially, and the other decays exponentially as the shape parameter c increases

$$\varepsilon \sim O\left(e^{ac}\lambda^{c/h}\right),\ 0<\lambda<1, a>0, \tag{2.14}$$

or

$$\varepsilon \sim O\left(e^{ac^2}\lambda^{c/h}\right),\ 0<\lambda<1, a>0. \tag{2.15}$$

Huang et al. [6] proposed an empirical error estimate for the IMQ RBF

$$\varepsilon \sim O\left(e^{ac^{3/2}}\lambda^{c^{1/2}/h}\right),\ 0<\lambda<1, a>0. \tag{2.16}$$

Following Madych's formula, Cheng [14] established the following estimate for the Gaussian RBF

$$\varepsilon \sim O\left(e^{ac^4}\lambda^{c/h}\right),\ 0<\lambda<1, a>0. \tag{2.17}$$

From the above-mentioned error estimates, one can derive different explicit formulas for the optimal c. According to Eq. (2.15), the optimal c can be approximated by

$$c_{\text{opt}} \sim O(-\ln\lambda/2ah). \tag{2.18}$$

Similar to Eq. (2.18), the optimal c for IMQ RBF in terms of Eq. (2.16) is

$$c_{\text{opt}} \sim O(-\ln\lambda/3ah). \tag{2.19}$$

The optimal c for Gaussian RBF can also be obtained from Eq. (2.17)

$$c_{\text{opt}} \sim O\left((-\ln\lambda)^{1/3}\Big/\left(2^{2/3}a^{1/3}h^{1/3}\right)\right). \tag{2.20}$$

In recent years, we have witnessed the continued efforts of many to establish the theory of evaluating the optimal shape parameter c in the MQ interpolation. However, such an explicit formula is only available in special cases. Consequently, numerically determining the optimal c proves to be essential. And numerical experiments find that the best c, via a numerical scheme, may not be theoretically optimal.

Since the condition number of the MQ interpolation matrix grows rapidly as c increases, the optimal c is the largest value at which it can be utilized before the instability of matrix calculation occurs due to the machine precision. We draw the following conclusions upon the above discussions.

Among the advantages of Globally-supported RBFs are

(a) Highly accurate and often converge exponentially.
(b) Easy to apply to high dimensional problems.
(c) Meshless in the approximation of multivariate scattered data, and easy to improve the numerical accuracy by adding more points around large gradient regions.

On the other hand, the downside is that the interpolation matrix is fully populated and ill-conditioned, and thus sensitive to shape parameter. As a result, it is computationally very expensive to apply the traditional RBF interpolation to large-scale problems.

Table 2.4 Wendland's CS-RBFs

Dimension	$\phi(\mathbf{x})$	Continuity of function
$d=1$	$(1-r)_+$	C^0
	$(1-r)_+^3(3r+1)$	C^2
	$(1-r)_+^5(8r^2+5r+1)$	C^4
$d=2,3$	$(1-r)_+^2$	C^0
	$(1-r)_+^4(4r+1)$	C^2
	$(1-r)_+^6(35r^2+18r+3)$	C^4
	$(1-r)_+^8(32r^3+25r^2+8r+1)$	C^6

2.1.2 Compactly-Supported RBFs

Following a similar methodology in the corrected reproducing kernel approximation [17], Wu [18] and Wendland [19] proposed a new type of RBFs to make the interpolation matrix sparse, which is defined as compactly-supported positive definite RBFs (CS-RBFs). The popular Wendland's CS-RBFs [19] are listed below in Table 2.4.

Note that the cut-off function $(r)_+$ is defined to be r if $0 \le r \le 1$ and to be zero elsewhere. Furthermore, another class of CS-RBFs constructed by Buhmann [20] is reminiscent of the popular thin plate splines. Three examples of these CS-RBFs are given below

$$\phi(\mathbf{x}) = \left(2r^4\log(r) - 7r^4/2 + 16r^3/3 - 2r^2 + 1/6\right)_+, \mathbf{x} \in R^3, \tag{2.21}$$

$$\phi(\mathbf{x}) = \left(112r^{9/2}/45 + 16r^{7/2}/3 - 7r^4 - 14r^2/15 + 1/9\right)_+, \mathbf{x} \in R^2, \tag{2.22}$$

$$\phi(\mathbf{x}) = \left(1/18 - r^2 + 4r^3/9 + r^4/2 - 4r^3\log(r)/3\right)_+, \mathbf{x} \in R^2. \tag{2.23}$$

Wu employs convolution to construct another kind of CS-RBFs as shown in Table 2.5. Wu's functions can be derived by the following formula

$$\varphi_{k,s} = D^k(\varphi_s), d \le 2k+1, \tag{2.24}$$

where differential operator D is defined as

Table 2.5 Wu's CS-RBFs

k	$\varphi_{k,3}(\mathbf{x})$	Continuity of function
0	$(1-r)_+^7\left(5r^6+35r^5+101r^4+147r^3+101r^2+35r+5\right)$	C^6
1	$(1-r)_+^6\left(5r^5+30r^4+72r^3+82r^2+36r+6\right)$	C^4
2	$(1-r)_+^5(5r^4+25r^3+48r^2+40r+8)$	C^2
3	$(1-r)_+^4(5r^3+20r^2+29r+16)$	C^0

$$(D\varphi)(r) = -\varphi'(r)/r, r \geq 0, \tag{2.25}$$

and the strictly positive definite function $\varphi_s(r)$ is stated as

$$\varphi_s(r) = (\varphi * \varphi)(2r) = \int_{-\infty}^{\infty} \left(1-t^2\right)_+^s \left(1-(2r-t)^2\right)_+^s dt. \tag{2.26}$$

The CS-RBFs can result in a sparse banded interpolation matrix and effectively avoids the ill-conditioned and dense matrix in the classical RBF interpolation and consequently reduces computational costs. However, the discouraging lower order of accuracy causes a major impediment to its practical use. To overcome the ill-conditioned problems and reduce the computational costs without loss of accuracy, several alternative localized approaches have been proposed and will be introduced in Chap. 3.

2.2 Problem-Dependent RBFs

As the RBF collocation methods attract growing attention in the field of numerical PDEs in the recent two decades, various solutions of PDEs and their variants emerge to be a powerful approach in the construction of the problem-dependent RBFs. This section introduces several problem-dependent RBFs. Consider the following elliptic PDEs

$$\begin{aligned} \Re u &= f(\mathbf{x}), \ \mathbf{x} \in \Omega, \\ Bu &= g(\mathbf{x}), \ \mathbf{x} \in \Gamma, \end{aligned} \tag{2.27}$$

where $\Re$ and B denote the linear partial differential operator and boundary operators. $\Omega \subset R^n$ is a bounded domain, and Γ denotes its boundary.

2.2.1 Fundamental Solutions

The fundamental solutions of radially invariant differential operator have the radial form with respect to origin and are of a radial function. The fundamental solution ϕ_F satisfies the governing differential equation of interest

$$\Re\{\phi_F\} = -\delta_i, \tag{2.28}$$

where δ_i is the Dirac delta function.

The fundamental solutions of commonly used differential operators are listed in Table 2.6 [21], where Δ denotes the Laplace operator, ∇ the gradient operator, D the diffusivity coefficient, λ a real number known as the wave number, $\mathbf{v}$ and $\mathbf{r}$ the velocity vector and distance vector, $\mu = \sqrt{(|\mathbf{v}|/2D)^2 + \lambda/D}$, κ foundation stiffness,

Table 2.6 Fundamental solutions to commonly used differential operators of two and three dimensions

$\Re$	2D	3D
Δ	$\ln(r)/(2\pi)$	$1/(4\pi r)$
$\Delta+\lambda^2$	$Y_0(\lambda r)/(2\pi)$	$\cos\lambda r/(4\pi r)$
$\Delta-\lambda^2$	$K_0(\lambda r)/(2\pi)$	$e^{-\lambda r}/(4\pi r)$
$D\Delta+\mathbf{v}\bullet\nabla-\lambda^2$	$K_0(\mu r)e^{-\frac{\mathbf{v}\bullet\mathbf{r}}{2D}}/(2\pi)$	$e^{-\mu r-\frac{\mathbf{v}\bullet\mathbf{r}}{2D}}/(4\pi r)$
$\Delta^2-\lambda^4$	$(Y_0(\lambda r)+K_0(\lambda r))/(2\pi)$	$\left(e^{-\lambda r}+\cos\lambda r\right)/(4\pi r)$
$\Delta^2+\kappa^2$	$Kei(\sqrt{\kappa}r)+Ber(\sqrt{\kappa}r)$	$Kei_{3/2}(\sqrt{\kappa}r)+Ber_{3/2}(\sqrt{\kappa}r)$
$\Delta^2-\lambda^2\Delta$	$\left(K_0(\lambda r)+\ln(r)\right)/\left(2\pi\lambda^2\right)$	$\left(e^{-\lambda r}+1\right)/\left(4\pi\lambda^2 r\right)$

and r the Euclidean norm between the point $\mathbf{x}$ and the origin. Y_0 and K_0 are the Bessel and modified Bessel functions of the second kind of order zero, respectively. We can see that the two Kelvin functions are the component functions of the fundamental solutions of the Winkler operator, where *Kei* represents the modified Kelvin functions of the second kind, and *Ber* denotes the Kelvin functions of the first kind. It is worthy noting that the fundamental solutions to a differential operator may not be unique. For the Laplace operator, a constant may be included in its fundamental solution.

By utilizing Green second identity, the high-order fundamental solutions of the Laplace operator Δ^m [22] can be derived by

$$\phi_F^m(\mathbf{x})=\begin{cases}\dfrac{r^{2m}}{2\pi}(C_m\ln r-B_m), & \mathbf{x}\in R^2\\ \dfrac{1}{(2m)!}\dfrac{r^{2m-1}}{4\pi}, & \mathbf{x}\in R^3\end{cases}, \tag{2.29}$$

where

$$C_0=1,\ B_0=0,\ C_{m+1}=\frac{C_m}{4(m+1)^2},\ B_{m+1}=\frac{1}{4(m+1)^2}\left(\frac{C_m}{m+1}+B_m\right).$$

Itagaki [23] and Chen [24] derived the explicit expressions of high-order fundamental solutions of Helmholtz, modified Helmholtz, and steady convection–diffusion operators. The high-order fundamental solutions of Helmholtz-type operator $\left(\Delta+\lambda^2\right)^m$ [23, 24] are given by

$$\phi_F^m(\mathbf{x})=A_m(\lambda r)^{m+1-n/2}Y_{m-1+n/2}(\lambda r),\quad \mathbf{x}\in R^n, \tag{2.30}$$

where $A_m=A_{m-1}/2m\lambda^2, A_0=1$, m is the order of operator of interest, and n denotes dimensionality.

The high-order fundamental solutions of modified Helmholtz-type operator $\left(\Delta-\lambda^2\right)^m$ [23, 24] are given by

$$\phi_F^m(\mathbf{x}) = A_m(\lambda r)^{m+1-n/2} K_{m-1+n/2}(\lambda r), \quad \mathbf{x} \in R^n. \tag{2.31}$$

The high-order fundamental solutions of modified convection–diffusion-type operator $\left(D\Delta + \mathbf{v} \bullet \nabla - \lambda^2\right)^m$ [24] are given by

$$\phi_F^m(\mathbf{x}) = A_m(\mu r)^{m+1-n/2} e^{-\frac{\mathbf{v} \bullet \mathbf{r}}{2D}} K_{m-1+n/2}(\mu r), \quad \mathbf{x} \in R^n. \tag{2.32}$$

Furthermore, the high-order composite operator is the product of different types of commonly used differential operators. For instance, the thin plate vibration operator is the product of the Laplace and the Helmholtz operators, and the Berger operator is a composite operator of the Laplace and the modified Helmholtz operators. And their fundamental solutions of orders are a sum of the solutions of the corresponding component operators. Recently, Chen [24] derived the high-order fundamental solutions of thin plate vibration, Berger plate, and Winkler plate. The high-order fundamental solutions of thin plate vibration-type operator $\left(\nabla^4 - \lambda^4\right)^m$ are given by

$$\phi_F^m(\mathbf{x}) = A_m(\lambda r)^{m+1-n/2} \left(Y_{m-1+n/2}(\lambda r) + K_{m-1+n/2}(\lambda r)\right), \quad \mathbf{x} \in R^n. \tag{2.33}$$

The high-order fundamental solutions of Berger plate-type operator $\left(\nabla^4 - \lambda^2 \nabla^2\right)^m$ are given by

$$\phi_F^m(\mathbf{x}) = \begin{cases} \dfrac{r^{2m}}{2\pi}(C_m \ln r - B_m) + A_m(\lambda r)^m K_m(\lambda r), & \mathbf{x} \in R^2 \\ \dfrac{1}{(2m)!}\dfrac{r^{2m-1}}{4\pi} + A_m(\lambda r)^{m-1/2} K_{m-1/2}(\lambda r), & \mathbf{x} \in R^3 \end{cases}. \tag{2.34}$$

The high-order fundamental solutions of Winkler plate-type operator $\left(\nabla^4 + \kappa^2\right)^m$ are given by

$$\phi_F^m(\mathbf{x}) = A_m\left(\sqrt{\kappa} r\right)^{m+1-n/2} \left(\mathrm{Kei}_{n/2}\left(\sqrt{\kappa} r\right) + \mathrm{Ber}_{n/2}\left(\sqrt{\kappa} r\right)\right), \quad \mathbf{x} \in R^n, \tag{2.35}$$

where m is an odd-integer order of operator, and

$$\phi_F^m(\mathbf{x}) = A_m\left(\sqrt{\kappa} r\right)^{m+1-n/2} \left(\mathrm{Kei}_{n/2-1}\left(\sqrt{\kappa} r\right) + \mathrm{Ber}_{n/2-1}\left(\sqrt{\kappa} r\right)\right), \quad \mathbf{x} \in R^n, \tag{2.36}$$

where m is an even-integer order. Note that we cannot verify the high-order Winkler plate-type fundamental solutions for more than 5-dimensions ($n > 5$) because of the following reasons:

(a) Equations (2.35) and (2.36) are not applicable for the Winkler operator of more than 5-dimensions.
(b) The solutions of the Winkler operator of more than 5-dimensions do not exist.

Table 2.7 Nonsingular RBF general solutions to commonly used differential operators

$\Re$	2D	3D
Δ	/	/
$\Delta+\lambda^2$	$J_0(\lambda r)/(2\pi)$	$\sin(\lambda r)/(4\pi r)$
$\Delta-\lambda^2$	$I_0(\lambda r)/(2\pi)$	$\sinh(\lambda r)/(4\pi r)$
$D\Delta+\mathbf{v}\bullet\nabla-\lambda^2$	$I_0(\mu r)e^{-\frac{\mathbf{v}\bullet\mathbf{r}}{2D}}/(2\pi)$	$e^{-\frac{\mathbf{v}\bullet\mathbf{r}}{2D}}\sinh(\mu r)/(4\pi r)$
$\nabla^4-\lambda^4$	$(J_0(\lambda r)+I_0(\lambda r))/(2\pi)$	$(\sin(\lambda r)+\sinh(\lambda r))/(4\pi r)$
$\nabla^4+\kappa^2$	$\mathrm{Bei}(\sqrt{\kappa}r)+\mathrm{Ber}(\sqrt{\kappa}r)$	$\mathrm{Bei}_{3/2}(\sqrt{\kappa}r)+\mathrm{Ber}_{3/2}(\sqrt{\kappa}r)$
$\nabla^4-\lambda^2\nabla^2$	$(I_0(\lambda r)+1)/(2\pi\lambda^2)$	$(\sinh(\lambda r)+r)/(4\pi\lambda^2 r)$

2.2.2 General Solutions

It is well known that the fundamental solutions have singularities at origin. Thereby, the special treatment of these singularities should be handled numerically. In contrast, Chen [24, 25] proposed the general solutions ϕ_G, which are nonsingular radial functions satisfying the corresponding governing differential equations in the manner

$$\Re\{\phi_G\}=0. \tag{2.37}$$

It is seen from Eq. (2.37) that the general solutions at origin have a bounded value rather than infinity as in the fundamental solution case. The general solutions of differential operator differ essentially from the corresponding fundamental solutions in that the former are nonsingular, while the latter are singular at origin.

Similarly, the nonsingular general solutions are also one kind of radial functions. Some useful general solutions [24] are listed in Table 2.7, where I_0 and J_0 represent the Bessel and modified Bessel functions of the first kind of order zero, respectively, and two Kelvin functions are the component functions of the general solutions of the Winkler operator, *Ber* and *Bei* denote the Kelvin functions of the first and second kind, respectively. It is noted that the RBF general solution of Laplace equation is a constant and is not suitable as a basis function. This issue will be further discussed in the next section.

We can also obtain the high-order RBF general solutions of Helmholtz-type operator $\left(\Delta+\lambda^2\right)^m$ [24]

$$\phi_G^m(\mathbf{x})=A_m(\lambda r)^{m+1-n/2}J_{m-1+n/2}(\lambda r),\quad \mathbf{x}\in R^n, \tag{2.38}$$

where $A_m=A_{m-1}/2m\lambda^2, A_0=1$, m denotes the order of operator, and n represents the dimensionality.

The high-order RBF general solutions of modified Helmholtz-type operator $\left(\Delta-\lambda^2\right)^m$ [24] are given by

$$\phi_G^m(\mathbf{x})=A_m(\lambda r)^{m+1-n/2}I_{m-1+n/2}(\lambda r),\quad \mathbf{x}\in R^n. \tag{2.39}$$

The high-order RBF general solutions of modified convection–diffusion-type operator $\left(D\Delta + \mathbf{v} \bullet \nabla - \lambda^2\right)^m$ [24] are represented by

$$\phi_G^m(\mathbf{x}) = A_m(\mu r)^{m+1-n/2} e^{-\frac{\mathbf{v}\bullet\mathbf{r}}{2D}} I_{m-1+n/2}(\mu r), \quad \mathbf{x} \in R^n. \tag{2.40}$$

The high-order RBF general solutions of thin plate vibration-type operator $\left(\nabla^4 - \lambda^4\right)^m$ are expressed as

$$\phi_G^m(\mathbf{x}) = A_m(\lambda r)^{m+1-n/2}\left(J_{m-1+n/2}(\lambda r) + I_{m-1+n/2}(\lambda r)\right), \quad \mathbf{x} \in R^n. \tag{2.41}$$

The high-order RBF general solutions of Berger plate-type operator $\left(\nabla^4 - \lambda^2\nabla^2\right)^m$ are stated as

$$\phi_G^m(\mathbf{x}) = A_m + A_m(\lambda r)^{m+1-n/2} I_{m-1+n/2}(\lambda r), \quad \mathbf{x} \in R^n. \tag{2.42}$$

The high-order RBF general solutions of Winkler plate-type operator $(\nabla^4 + \kappa^2)^m$ are given by

$$\phi_G^m(\mathbf{x}) = A_m\left(\sqrt{\kappa} r\right)^{m+1-n/2}\left(\mathrm{Bei}_{n/2}\left(\sqrt{\kappa} r\right) + \mathrm{Ber}_{n/2}\left(\sqrt{\kappa} r\right)\right), \quad n = 2, 3, \tag{2.43}$$

where the order m of operator is an odd integer, and

$$\phi_G^m(\mathbf{x}) = A_m\left(\sqrt{\kappa} r\right)^{m+1-n/2}\left(\mathrm{Bei}_{n/2-1}\left(\sqrt{\kappa} r\right) + \mathrm{Ber}_{n/2-1}\left(\sqrt{\kappa} r\right)\right), \; n = 2, 3, \tag{2.44}$$

where m is an even integer. It should also be mentioned that Eqs. (2.43) and (2.44) do not establish for the Winkler operators of more than 3-dimensions. It remains an open issue to find such high-order general solutions.

2.2.3 Harmonic Functions

As mentioned earlier, the general solution of Laplace equation is a constant rather than a RBF and is not suitable for function interpolation and numerical PDEs. Chen [26] made an attempt to use the nonsingular general solutions of Helmholtz-like equation with a small characteristic parameter to replace the constant general solution of Laplace equation. However, the characteristic parameter such as the wave number should generally be small to get accurate solution. It is somewhat sensitive to the domain geometry of problem of interest. And it is not easy to determine its optimal value as the shape parameter of the MQ.

On the other hand, Hon and Wu [27] applied a translate-invariant 2D harmonic function as the basis function to devise a simple and efficient numerical scheme for solving 2D Laplace problems. Hon and Wu's harmonic function of the two-dimensional Laplace equation $\Delta\left(H_2^0(x_i, y_i)\right) = 0$ is given by

$$H_2^0(x_i, y_i) = \exp(-c(x_{ik}^2 - y_{ik}^2))\cos(2cx_{ik}y_{ik}), \tag{2.45}$$

where c is the shape parameter and is dependent on problem of interest, and $x_{ik} = x_i - x_k$, $y_{ik} = y_i - y_k$.

Compared with the singular fundamental solutions, the harmonic solutions are nonsingular. Thus, it is appealing to choose harmonic functions, which avoid the singularities of Laplace fundamental solution. However, this comes at a price one has to pay that their shape parameter c has to be determined as the MQ shape parameter [28]. The performances such as accuracy and convergence rate of the harmonic functions are largely dependent on the problem-dependent parameter c.

The harmonic functions are guaranteed invertibility if the solution is in the bounded domain or decays to zero at infinite for the unbounded domain. As quoted from Hon and Wu [27], "The result in this paper is given for bounded functions which are harmonic on the upper half plane. This ensures that the functions can be expressed in the form of Poisson integrals so that the solution can be determined by its given values on the boundary. The numerical computations, however, indicate that the result is also valid for unbounded functions (but bounded on the boundary) which are harmonic on the upper half plane."

High-order polyharmonic solutions

Based on Hon and Wu's work [27], the high-order polyharmonic functions in two- and three- dimensional problems are constructed by Chen and Fu [29, 30]. The m-order polyharmonic functions of $\Delta^m\left(H_2^m(x_i, y_i)\right) = 0$ in two-dimension are represented as

$$H_2^m(x_i, y_i) = r^{2m} \exp\left(-c\left(x_{ik}^2 - y_{ik}^2\right)\right) \cos(2cx_{ik}y_{ik}). \tag{2.46}$$

Three-dimensional harmonic solutions

The harmonic function of three-dimensional Laplace equation $\Delta\left(H_3^0(x_i, y_i, z_i)\right) = 0$ can be intuitionally obtained as

$$\begin{aligned} H_3^0(x_i, y_i, z_i) = {} & \exp\left(-c\left(x_{ik}^2 - y_{ik}^2\right)\right) \cos(2cx_{ik}y_{ik}) + \\ & \exp\left(-c\left(y_{ik}^2 - z_{ik}^2\right)\right) \cos(2cy_{ik}z_{ik}) + \exp\left(-c\left(z_{ik}^2 - x_{ik}^2\right)\right) \cos(2cz_{ik}x_{ik}) \end{aligned} \tag{2.47}$$

Similarly, the m-order polyharmonic functions of $\Delta^m\left(H_3^m(x_i, y_i, z_i)\right) = 0$ in three dimension are represented as

$$\begin{aligned} H_3^m(x_i, y_i, z_i) = {} & r^{2m}\left\{\exp\left(-c\left(x_{ik}^2 - y_{ik}^2\right)\right) \cos(2cx_{ik}y_{ik}) + \right. \\ & \left. \exp\left(-c\left(y_{ik}^2 - z_{ik}^2\right)\right) \cos(2cy_{ik}z_{ik}) + \exp\left(-c\left(z_{ik}^2 - x_{ik}^2\right)\right) \cos(2cz_{ik}x_{ik})\right\} \end{aligned} \tag{2.48}$$

2.2.4 Particular Solutions

Another important type of problem-dependent RBFs are particular solutions. A splitting approach [31] is used to split the solution of the nonhomogeneous governing Eq. (2.27) into homogeneous solution and particular solution. The key issue is to construct the particular solutions $\Phi(r)$ to satisfy the following equation

$$\Re\Phi(r) = \phi(r). \tag{2.49}$$

Typically, there are two approaches to construct the particular solutions $\Phi(r)$. The first approach is utilizing the above-mentioned RBFs as the particular solutions $\Phi(r)$, then deriving the basis functions $\phi(r)$ from Eq. (2.49) by differentiation process. This scheme is easy to derive the particular solutions, however, such RBFs $\phi(r)$ may not remain in the positive definite property to guarantee the matrix invertibility, which depends on the governing differential operator $\Re$.

The second approach is utilizing the existing RBFs discussed before as the functions $\phi(r)$, then deriving the particular solutions $\Phi(r)$ from Eq. (2.49) by reverse differentiation process. The deriving process in this strategy is far more challenging than the former one. Nevertheless, the corresponding derived particular solutions $\Phi(r)$ inherit the positive definite property from the existing RBFs. In virtue of this excellent property, various particular solutions have been derived by the second approach. Chen and Rashed [32] were the first to extend the derivation of TPS-based solutions for Helmholtz-type operators. Muleshkov et al. [33] and Cheng [34] further derived the particular solutions by Polyharmonic splines. Recently, Muleshkov and Golberg [35], Chen et al. [36], and Tsai et al. [37] extended the derivation to more composite differential operators. We list some particular solutions $\Phi(r)$ for the traditional RBFs $\phi(r)$ [38] as follows:

(a) The corresponding particular solutions as a prior to satisfy the differential equation $\Delta\Phi(r) = \phi(r)$.

For MQ, $\phi(r) = \sqrt{r^2 + c^2}$, we have the following results

$$\Phi(r) = \frac{4c^2 + r^2}{9}\sqrt{c^2 + r^2} - \frac{c^3}{3}\ln\left(c + \sqrt{c^2 + r^2}\right) \tag{2.50}$$

in R^2, and

$$\Phi(r) = \begin{cases} \frac{5c^2+2r^2}{24}\sqrt{c^2 + r^2} + \frac{c^4 \ln\left(r+\sqrt{c^2+r^2}\right)}{8r} - \frac{c^3}{3} - \frac{c^4 \ln(c)}{8r}, r \neq 0 \\ 0,\ r = 0 \end{cases} \tag{2.51}$$

in R^3.

For IMQ, $\phi(r) = 1/\sqrt{r^2 + c^2}$, we obtain

$$\Phi(r) = \sqrt{c^2 + r^2} - c\ln\left(c + \sqrt{c^2 + r^2}\right) \tag{2.52}$$

in R^2, and

$$\Phi(r) = \begin{cases} \frac{\sqrt{c^2+r^2}}{2} + \frac{c^2}{2r}\ln\left(\frac{r+\sqrt{c^2+r^2}}{c}\right) - \frac{c}{2}, r \neq 0 \\ 0,\ r = 0 \end{cases} \tag{2.53}$$

in R^3.

For Polyharmonic splines $\phi(r) = r^k \ln(r), k = 2, 4, 6, \ldots$, in R^2, we derive

$$\Phi(r) = \frac{r^{k+2}\ln(r)}{4(k/2+1)^2} - \frac{r^{k+2}}{4(k/2+1)^3}, \tag{2.54}$$

which can be regarded as high-order fundamental solutions of Laplace operator.

For Polyharmonic splines, $\phi(r) = r^k, k = 1, 3, 5, \ldots$, in R^3, we get

$$\Phi(r) = \frac{r^{k+3}}{(k+3)(k+2)}. \tag{2.55}$$

(b) The corresponding particular solutions as a prior to satisfy the differential equation $\left(\Delta + \lambda^2\right)\Phi(r) = \phi(r)$.

For TPS, $\phi(r) = r^2\ln(r)$ in R^2, we have the following results

$$\Phi(r) = \begin{cases} -\frac{r^2\ln(r)}{\lambda^2} + \frac{4\ln(r)+4}{\lambda^4} + \frac{4}{\lambda^4}K_0(\lambda r), r \neq 0 \\ \frac{4}{\lambda^4} - \frac{4\gamma}{\lambda^4} - \frac{4}{\lambda^4}\ln\left(\frac{\lambda}{2}\right), \ r = 0 \end{cases}. \tag{2.56}$$

For Polyharmonic splines of order two, $\phi(r) = r^4\ln(r)$ in R^2, we derive the following results

$$\Phi(r) = \begin{cases} -\frac{r^4\ln(r)}{\lambda^2} + \frac{8r^2(2\ln(r)+1)}{\lambda^4} + \frac{64\ln(r)+96}{\lambda^6} + \frac{64K_0(\lambda r)}{\lambda^6}, r \neq 0 \\ \frac{96}{\lambda^6} - \frac{64\gamma}{\lambda^6} - \frac{64}{\lambda^6}\ln\left(\frac{\lambda}{2}\right), \ r = 0 \end{cases}. \tag{2.57}$$

For Polyharmonic splines of higher order, $\phi(r) = r^k\ln(r), k = 4, 6, 8, \cdots$ in R^2, we get

$$\Phi(r) = -\frac{1}{\lambda^2}\sum_{i=0}^{k/2}\left(-\frac{\Delta}{\lambda^2}\right)^i r^k\ln(r) - \frac{(-1)^{k/2}(k)!!^2}{\lambda^{k+2}}K_0(\lambda r). \tag{2.58}$$

For TPS $\phi(r) = r$ in R^3, we find the following particular solution

$$\Phi(r) = \begin{cases} -\frac{r}{\lambda^2} + \frac{2}{\lambda^4 r} - \frac{2e^{-\lambda r}}{\lambda^4 r}, r \neq 0 \\ \frac{2}{\lambda^3}, r = 0 \end{cases}. \tag{2.59}$$

For Polyharmonic splines $\phi(r) = r^k, k = 1, 3, 5, \cdots$ in R^3, we derive the particular solution

$$\Phi(r) = -\sum_{i=0}^{k/2}\frac{(-1)^i(k+1)!r^{k-2i}}{(k+1-2i)!\lambda^{2i+2}} + \frac{2(-1)^i(k+1)!}{\lambda^{2k+4}}\frac{e^{-\lambda r}}{r}. \tag{2.60}$$

(c) The corresponding particular solutions as a prior to satisfy the differential equation $\left(\Delta - \lambda^2\right)\Phi(r) = \phi(r)$.

For TPS $\phi(r) = r^2\ln(r)$ in R^2, we obtain

$$\Phi(r)=\begin{cases}-\frac{r^2\ln(r)}{\lambda^2}-\frac{4\ln(r)+4}{\lambda^4}-\frac{4}{\lambda^4}K_0(\lambda r), r\neq 0\\ -\frac{4}{\lambda^4}+\frac{4\gamma}{\lambda^4}+\frac{4}{\lambda^4}\ln\left(\frac{\lambda}{2}\right), r=0\end{cases}. \tag{2.61}$$

For Polyharmonic splines of order 2, $\phi(r)=r^4\ln(r)$ in R^2, the corresponding particular solution is

$$\Phi(r)=\begin{cases}-\frac{r^4\ln(r)}{\lambda^2}-\frac{8r^2(2\ln(r)+1)}{\lambda^4}-\frac{64\ln(r)+96}{\lambda^6}-\frac{64K_0(\lambda r)}{\lambda^6}, r\neq 0\\ -\frac{96}{\lambda^6}+\frac{64\gamma}{\lambda^6}+\frac{64}{\lambda^6}\ln\left(\frac{\lambda}{2}\right), r=0\end{cases}. \tag{2.62}$$

For Polyharmonic splines of higher order $\phi(r)=r^k\ln(r), k=4,6,8,\cdots$ in R^2, we have

$$\Phi(r)=-\frac{1}{\lambda^2}\sum_{i=0}^{k/2}\left(\frac{\Delta}{\lambda^2}\right)^i r^k\ln(r)-\frac{(k)!!^2}{\lambda^{k+2}}K_0(\lambda r). \tag{2.63}$$

For TPS $\phi(r)=r$ in R^3, we get

$$\Phi(r)=\begin{cases}-\frac{r}{\lambda^2}-\frac{2}{\lambda^4 r}+\frac{2e^{-\lambda r}}{\lambda^4 r}, r\neq 0\\ -\frac{2}{\lambda^3}, r=0\end{cases}. \tag{2.64}$$

For Polyharmonic splines $\phi(r)=r^k, k=1,3,5,\cdots$ in R^3, we obtain

$$\Phi(r)=-\sum_{i=0}^{k/2}\frac{(k+1)!r^{k-2i}}{(k+1-2i)!\lambda^{2i+2}}+\frac{2(k+1)!}{\lambda^{k+3}}\frac{e^{-\lambda r}}{r}. \tag{2.65}$$

(d) The corresponding particular solutions as a prior to satisfy the differential equation $\Delta^2\Phi(r)=\phi(r)$.

For MQ, $\phi(r)=\sqrt{r^2+c^2}$ in R^2, we derive the particular solution

$$\begin{aligned}\Phi(r)=&\frac{1}{12}r^2c^3-\frac{7}{60}c^4\sqrt{c^2+r^2}+\frac{2}{45}c^2\left(c^2+r^2\right)^{\frac{3}{2}}\\ &+\frac{1}{225}c^2\left(c^2+r^2\right)^{\frac{5}{2}}+\frac{2c^2-5r^2}{60}\ln\left(c+\sqrt{c^2+r^2}\right)\end{aligned} \tag{2.66}$$

For IMQ, $\phi(r)=1/\sqrt{r^2+c^2}$ in R^2, the particular solution is stated as

$$\Phi(r)=\begin{cases}-\frac{5c^2\sqrt{c^2+r^2}}{12}+\frac{\left(c^2+r^2\right)^{\frac{3}{2}}}{9}+\frac{cr^2}{2}+\frac{\left(2c^3-3cr^2\right)\ln\left(c+\sqrt{c^2+r^2}\right)}{12}, r\neq 0\\ \frac{c^3}{36}(6\ln(2c)-11), r=0\end{cases}. \tag{2.67}$$

For Polyharmonic splines $\phi(r)=r^k, k=1,3,5,\cdots$ in R^3, we have

$$\Phi(r)=\frac{r^{k+4}}{(k+2)(k+3)(k+4)(k+5)} \tag{2.68}$$

(e) The corresponding particular solutions as a prior to satisfy the differential equation $\left(\nabla^4 - \lambda^4\right)\Phi(r) = \phi(r)$.

For Polyharmonic splines of order 2, $\phi(r) = r^4 \ln(r)$ in R^2, we get

$$\Phi(r) = \begin{cases} -\frac{r^4 \ln(r)}{\lambda^4} - \frac{64\ln(r)+96}{\lambda^8} - \frac{16(K_0(\lambda r) - \pi Y_0(\lambda r))}{\lambda^8}, r \neq 0 \\ -\frac{96}{\lambda^8} + \frac{64\gamma}{\lambda^8} + \frac{64}{\lambda^8}\ln\left(\frac{\lambda}{2}\right), \ r = 0 \end{cases}. \tag{2.69}$$

For Polyharmonic splines$\phi(r) = r^k \ln(r), k = 2, 4, 6, \cdots$ in R^2, we obtain

$$\Phi(r) = -\frac{1}{\lambda^4}\sum_{i=0}^{k/2}\left(\frac{\Delta^2}{\lambda^4}\right)^i r^k \ln(r) - \frac{(k/2)!^2}{\lambda^{k+4}}\left(2K_0(\lambda r) + (-1)^{k/2+1}\pi Y_0(\lambda r)\right). \tag{2.70}$$

For Polyharmonic splines $\phi(r) = r^k, k = 1, 3, 5, \cdots$ in R^3, we have

$$\Phi(r) = -\frac{1}{\lambda^4}\sum_{i=0}^{(k-1)/2}\left(\frac{\Delta^2}{\lambda^4}\right)^i r^{k+2} + \frac{(k+1)!}{2\lambda^{k+5} r}\left(e^{-\lambda r} + (-1)^{(k+1)/2}\cos(\lambda r)\right). \tag{2.71}$$

(f) The corresponding particular solutions as a prior to satisfy the differential equation $(\nabla^4 + \kappa^2)\Phi(r) = \phi(r)$.

For Polyharmonic splines $\phi(r) = r^k \ln(r), k = 2, 4, 6, \cdots$ in R^2, we have the following results

$$\Phi(r) = \frac{\sum_{i=0}^{k/2}\left(-\frac{\Delta^2}{\kappa^2}\right)^i r^k \ln(r)}{\kappa^2} + \frac{(-1)^{k/2}(k/2)!^2\left(2K_0(\sqrt{\kappa}r) + (-1)^{k/2+1}\pi Y_0(\sqrt{\kappa}r)\right)}{\kappa^{k/2+2}}. \tag{2.72}$$

For Polyharmonic splines $\phi(r) = r^k, k = 1, 3, 5, \cdots$ in R^3, we have

$$\Phi(r) = \frac{\sum_{i=0}^{(k-1)/2}\left(-\frac{\Delta^2}{\kappa^2}\right)^i r^{k+2}}{\kappa^2} + \frac{(-1)^{\frac{k+1}{2}}(k+1)!\left(e^{-\sqrt{\kappa}r} + (-1)^{\frac{k+1}{2}}\cos(\sqrt{\kappa}r)\right)}{2\kappa^{(k+5)/2} r} \tag{2.73}$$

2.2.5 Anisotropic RBFs

Numerical methods based on RBFs appear very efficient for isotropic problems. However, Carlson and Foley [39] found that the isotropic RBFs, such as the MQ and TPS, do not work well for the so-called track or directional data problems. This kind of problems characterizes a preferred direction. For directional data, the anisotropic RBFs can capture the directional property. For instance, consider heat conduction in anisotropic media

$$\sum_{i,j=1}^{d} \frac{\partial}{\partial x_i}\left(K_{ij}\frac{\partial u(\mathbf{x})}{\partial x_j}\right) = 0,\ \mathbf{x} \in \Omega, \tag{2.74}$$

where d denotes the dimensionality of problem. $K = \left[K_{ij}\right]_{1 \le i,j \le d}$ denotes the matrix of anisotropic material parameter, which has the symmetrical and positive-definite properties, for example, $d = 2$, $K_{12} = K_{21}$and $\Delta_K = \det(K) = K_{11}K_{22} - K_{12}^2 > 0$. Typically, there are two approaches to construct the anisotropic RBFs.

Domain mapping method [40]

The domain mapping method is a transformation technique and can be applied to the anisotropic problem in field theory. The 2D and 3D direct domain mapping formulas are represented by

$$\begin{pmatrix} X_1 - X_{k1} \\ X_2 - X_{k2} \end{pmatrix} = \begin{pmatrix} \sqrt{\Delta_K}/K_{11} & 0 \\ -K_{12}/K_{11} & 1 \end{pmatrix} \begin{pmatrix} x_1 - x_{k1} \\ x_2 - x_{k2} \end{pmatrix}, \tag{2.75}$$

$$\begin{pmatrix} X_1 - X_{k1} \\ X_2 - X_{k2} \\ X_3 - X_{k3} \end{pmatrix} = \begin{pmatrix} \sqrt{\Delta_K}/K_{11} & 0 & 0 \\ -K_{12}/K_{11} & 1 & 0 \\ \beta_1 & \beta_2 & \beta_3 \end{pmatrix} \begin{pmatrix} x_1 - x_{k1} \\ x_2 - x_{k2} \\ x_3 - x_{k3} \end{pmatrix}, \tag{2.76}$$

where

$\beta_1 = (K_{12}K_{13} - K_{23}K_{11})/\sqrt{w}$, $\beta_2 = (K_{12}K_{23} - K_{13}K_{22})/\sqrt{w}$, $\beta_3 = \Delta_K/\sqrt{w}$, and $w = K_{11}K_{33}\Delta_K - K_{11}K_{22}K_{13}^2 + 2K_{11}K_{12}K_{13}K_{23} - K_{23}^2K_{11}^2$.

Geodesic distance functions [41]

Another strategy is to construct geodesic distance functions. The standard Euclidean distance $r_k = \|\mathbf{x} - \mathbf{x}_k\|_2$ is replaced by the geodesic distance R_k between points $\mathbf{x} = (x_1, x_2, \cdots, x_d)$ and $\mathbf{x}_k = (x_{k1}, x_{k2}, \cdots, x_{kd})$ defined as below

$$R_k^2 = \sum_{i=1}^{d}\sum_{j=1}^{d} K_{ij}^{-1}(x_i - x_{ki})(x_j - x_{kj}) = (\mathbf{x} - \mathbf{x}_k)^T K^{-1}(\mathbf{x} - \mathbf{x}_k), \tag{2.77}$$

where $K^{-1} = \left[K_{ij}^{-1}\right]$ is the inverse anisotropic coefficient matrix. In case of isotropic media, K is an identity matrix and the geodesic distance is reduced to the Euclidean distance.

It is straightforward to construct the anisotropic RBFs from the corresponding isotropic RBFs described above via the variable transformation Eqs. (2.75), (2.76), and (2.77).

2.2.6 Time–Space RBFs

In terms of generalized time–space field, an interesting and significant extension of the RBF concept is to introduce time–space RBFs for time-dependent problems. One of the proposed methodology defines the interpolation function on

$R^n \times T$ [42], where T is the additional time axis. Hence the time–space RBFs have the representation form $\sqrt{r^2 + c^2|t|^2}$. The parameter c reflects a realistic relationship between space and time. Such a metric considers the time axis being "orthogonal" to all of the space axes but with a different unit.

Yet another type of the time–space RBFs originates from transient fundamental solution and general solution of time-dependent partial differential equations [43–45]. Consider the diffusion equation

$$\frac{\partial u(\mathbf{x}, t)}{\partial t} = k\nabla^2 u(\mathbf{x}, t),\ \mathbf{x} \in \Omega \subset R^n, \tag{2.78}$$

where $\mathbf{x}$ is the general spatial coordinate, t the time, k the diffusion coefficient. By applying the Fourier and the inverse Fourier transforms to Eq. (2.78), the fundamental solutions in R^n and the general solutions in R^3 can be obtained, respectively, and stated as

$$\phi_F^m(\mathbf{x}, t, \mathbf{s}, \tau) = \frac{e^{\frac{-\|\mathbf{x}-\mathbf{s}\|_2^2}{4k(t-\tau)}}}{(4k\pi(t-\tau))^{n/2}} H(t-\tau), \mathbf{x} \in R^n, \tag{2.79}$$

$$\phi_G^m(\mathbf{x}, t, \mathbf{s}, \tau) = e^{-k(t-\tau)} \frac{\sin\|\mathbf{x}-\mathbf{s}\|_2}{\|\mathbf{x}-\mathbf{s}\|_2}, \mathbf{x} \in R^3, \tag{2.80}$$

where n is the spatial dimensionality and $H(t)$ represents the Heaviside step function, $\mathbf{x}$ denotes the location of the field points, and $\mathbf{s}$ means the location of the source points. t and τ are the time of the field and source points, respectively.

2.3 Kernel RBFs

As the motto goes "the laws of universe are written in the language of partial differential equation," the construction of an efficient and stable RBF is not an exception. Building on the firm grounds of integral equation theory (distribution theory), this section presents a recent approach for constructing the novel RBFs in terms of the potential theory.

The Green second identity was found to be a powerful alternative tool to create and analyze efficient RBFs [43, 46, 47]. The kernel solutions of partial differential equations can be used to create the kernel RBFs. By using the Green second theorem, the solution of Eq. (2.27) can be expressed as

$$u(\mathbf{x}) = \int_\Omega f(\mathbf{s}) u^*(\mathbf{x}, \mathbf{s}) d\Omega(\mathbf{s}) + \int_\Gamma \left\{ u \frac{\partial u^*(\mathbf{x}, \mathbf{s})}{\partial n(\mathbf{s})} - \frac{\partial u}{\partial n(\mathbf{s})} u^*(\mathbf{x}, \mathbf{s}) \right\} d\Gamma(\mathbf{s}), \tag{2.81}$$

where u^* represents the fundamental solutions of governing operator $\Re$, and $\mathbf{s}$ denotes source point. It is noted that the first and second terms of Eq. (2.81) are the

particular and the homogeneous solutions in the PDE splitting approach [31]. Applying a numerical integral scheme to approximate Eq. (2.81), we have

$$u(\mathbf{x}) = \sum_{j=1}^{N} w(\mathbf{x}, \mathbf{x}_j) f(\mathbf{x}_j) u^* + \sum_{j=N_i+1}^{N} w(\mathbf{x}, \mathbf{x}_j) \left[u \frac{\partial u^*}{\partial n} - \frac{\partial u}{\partial n} u^* \right], \tag{2.82}$$

where N_i is the number of the interior knots in Ω, N the total number of knots in the domain and on the boundary, and $w(\mathbf{x}, \mathbf{x}_j)$ the integration weighting functions. We can further restate the approximate representation (2.82) as

$$u(\mathbf{x}) = \sum_{j=1}^{N} \alpha_j h_j(\mathbf{x}, \mathbf{x}_j) u^* f(\mathbf{x}_j) - \sum_{j=N_i+1}^{N} \beta_j p_j(\mathbf{x}, \mathbf{x}_j) u^* + \sum_{j=N_i+1}^{N} \gamma_j q_j(\mathbf{x}, \mathbf{x}_j), \tag{2.83}$$

where $\{\alpha_j\}, \{\beta_j\}$ and $\{\gamma_j\}$ are unknown expansion coefficients, $\{h_j\}$ and $\{p_j\}$ represents weighting functions to be specified. hu^*f, pu^* are in fact the radial basis functions. Therefore, the first term of Eq. (2.83) suggests that the RBFs can be constructed using interior source points $\{\mathbf{x}_j\}$ [43, 46, 47] by

$$\phi(\mathbf{x}, \mathbf{x}_j) = h_j(\mathbf{x}, \mathbf{x}_j) u^*(\mathbf{x}, \mathbf{x}_j) f(\mathbf{x}_j). \tag{2.84}$$

When u^* is a singular fundamental solution, h_j is an augmented RBF function to remove the singularities of fundamental solutions and guarantee that the function $\phi(x, x_j)$ has enough differentiability. Power function $h_j = r^m$ is a convenient choose where r denotes the Euclidean distance. For instance, the TPS is a special case of the kernel RBFs for 2D biharmonic operator. Polyharmonic splines RBFs are recommended for higher dimensional problems. On the other hand, u^* in Eq. (2.84) can be replaced by nonsingular general solutions [46, 48].

Regarding the boundary source points, we suggest a RBF as

$$\phi(\mathbf{x}, \mathbf{x}_j) = p_j(\mathbf{x}, \mathbf{x}_j) u^*(\mathbf{x}, \mathbf{x}_j). \tag{2.85}$$

The weighting function $p_j = r^m$ is also a simple choice. It is of worthy noting that the high-order fundamental solutions, general solutions, and harmonic functions in Sects. 2.2.1–2.2.3 are not singular and appear similar to the fundamental solutions augmented with a power function. Table 2.8 lists some typical kernel RBFs augmented by a power function [43].

Another strategy is to construct shifted kernel RBFs [43] by replacing Euclidean distance r in the fundamental solutions with a shifted distance variable $\sqrt{c^2 + r^2}$ to remedy the singularity, where c is a dilution shape parameter. For instance, the MQ RBF can be used as a correcting function to determine local optimal shape parameter by establishing the reproducing conditions. These shifted kernel RBFs are especially attractive for multiscale problems. Table 2.9 lists some shifted kernel RBFs.

Table 2.8 Kernel RBFs augmented by a power function

Power augmented scheme	$\phi(\mathbf{x})$
Polyharmonic spline	$\begin{cases} r^m, m = 1, 3, 5, \cdots \\ r^m \ln(r), m = 2, 4, 6, \cdots \end{cases}$
Thin plate spline	$r^2 \ln(r)$
Power exponential functions	$r^m e^{-r^2}$
High-order fundamental solutions	See Sect. 2.2.1
High-order RBF general solutions	See Sect. 2.2.2
High-order harmonic functions	See Sect. 2.2.3

With the help of the kernel solutions of time-dependent PDEs, we can also construct the time–space kernel RBFs. For instance, consider the wave propagation equation

$$\frac{\partial^2 u}{\partial x^2} = \frac{1}{c^2}\frac{\partial^2 u}{\partial t^2} + f(x,t). \tag{2.86}$$

Let

$$s = ict, \tag{2.87}$$

where $i = \sqrt{-1}$. We have

$$\frac{\partial^2 u}{\partial x^2} + \frac{\partial^2 u}{\partial s^2} = f(x,t). \tag{2.88}$$

Similar to the definition of Euclidean distance, the generalized time–space distance is defined by

$$r_j = \sqrt{(x-x_j)^2 + (s-s_j)^2} = \sqrt{(x-x_j)^2 - c^2(t-t_j)^2}. \tag{2.89}$$

However, such a definition can lead to complex value of distance variable. Thus, it is better to use

$$r_j = \sqrt{(x-x_j)^2 + c^2(t-t_j)^2}. \tag{2.90}$$

Table 2.9 Shifted kernel RBFs

Shape parameter scheme	$\phi(\mathbf{x})$
Multiquadric	$\sqrt{r^2 + c^2}$
Shifted logarithm function	$\ln\left(\sqrt{r^2 + c^2}\right)$
Shifted Polyharmonic spline	$r^m \ln\left(\sqrt{r^2 + c^2}\right)$
Shifted exponential function	$e^{-\sqrt{r^2+c^2}}$
Shifted fundamental solutions	$\phi_F^m(\sqrt{r^2 + c^2})$
Shifted RBF general solutions [49]	$\phi_G^m(\sqrt{r^2 + c^2})$

Here c is the wave velocity. The RBFs with respect to time–space distance (2.90) differ from the standard RBFs in that the time variable is handled equally as the space variables. Time–space RBFs eliminate time dependence directly in the basis functions. The Green second theory suggests that the time–space kernel RBFs can be constructed by [46, 47]

$$\phi(r_j) = h_j(r_j)u^*\left(r_j\right)f(\mathbf{x}_j, t), \tag{2.91}$$

for interior source points, and

$$\phi(r_j) = p_j(r_j)u^*\left(r_j\right), \tag{2.92}$$

for boundary source points.

Another strategy is to construct time-dependent kernel RBFs by augmenting fundamental or general solutions with time power function stated below

$$\phi(r_j) = t^{2m}u^*\left(r_j\right)f(\mathbf{x}_j, t), \tag{2.93}$$

where t^{2m} remedies the singularities of transient fundamental solution $u^*\left(r_j\right)$. The time–space RBFs in Sect. 2.2.6 can be modified by utilizing shifted RBF formulas (2.91–2.93). The time–space kernel RBFs have great potential to transient image data processing such as motion pictures.

The other approaches for constructing the appropriate RBFs are also reported in literatures, such as combined RBFs [50], oscillatory RBFs [51], Trefftz RBFs [52], and wavelet-based adaptive RBF method [53]. For more details, the interested readers may look into the respective papers.

References

1. E. Folio, Distance Transform. In: Technical Report no 0806, revision 1748. Laboratoire de Recherche et Dveloppement de l'Epita (Le Kremlin-Bictre cedex-France, 2008)
2. M.D. Buhmann, *Radial Basis Function: Theory and Implementations* (Cambridge University Press, Cambridge, 2003)
3. R. Franke, Scattered data interpolation: tests of some method. Math. Comput. **38**(157), 181–200 (1982)
4. J.G. Wang, G.R. Liu, On the optimal shape parameters of radial basis function used for 2-D meshless methods. Comput. Methods Appl. Mech. Eng. **191**(23–24), 2611–2630 (2002)
5. A.H.D. Cheng, M.A. Golberg, E.J. Kansa, G. Zammito, Exponential convergence and H-c multiquadric collocation method for partial differential equations. Numer. Methods Part. Differ. Eq. **19**(5), 571–594 (2003)
6. C.S. Huang, C.F. Lee, A.H.D. Cheng, Error estimate, optimal shape factor, and high precision computation of multiquadric collocation method. Eng. Anal. Boundary Elem. **31**(7), 614–623 (2007)
7. C.M.C. Roque, A.J.M. Ferreira, Numerical experiments on optimal shape parameters for radial basis function. Numer. Methods Part. Differ. Eq. **26**(3), 675–689 (2010)
8. B. Fornberg, C. Piret, On choosing a radial basis function and a shape parameter when solving a convective PDE on a sphere. J. Comput. Phys. **227**(5), 2758–2780 (2008)

9. J. Duchon, Interpolation des fonctions de deux variables suivant le principe de la flexion des plaques minces. Revue Francaise D Automatique Informatique Recherche Operationnelle **10**(12), 5–12 (1976)
10. W.R. Madych, S.A. Nelson, Multivariate interpolation and conditionally positive definite functions. Approx. Theor. Appl. **4**, 77–89 (1988)
11. W.R. Madych, S.A. Nelson, Multivariate interpolation and conditionally positive definite functions. 2. Math. Comput. **54**(189), 211–230 (1990)
12. W.R. Madych, S.A. Nelson, Bounds on multivariate polynomials and exponential error-estimates for multiquadric interpolation. J. Approx. Theor. **70**(1), 94–114 (1992)
13. Z.M. Wu, R.S. Schaback, Local error-estimates for radial basis function interpolation of scattered data. IMA J. Numer. Anal. **13**(1), 13–27 (1993)
14. A.H.D. Cheng, Multiquadric and its shape parameter-A numerical investigation of error estimate, condition number, and round-off error by arbitrary precision computation. Eng. Anal. Boundary Elem. **36**, 220–239 (2012)
15. H. Wendland, *Scattered Data Approximation* (Cambridge University Press, Cambridge, 2005)
16. W.R. Madych, Miscellaneous error-bounds for multiquadric and related interpolators. Comput. Math. Appl. **24**(12), 121–138 (1992)
17. W.K. Liu, J. Sukky, Multiple-scale reproducing kernel particle methods for large deformation problems. Int. J. Numer. Meth. Eng. **41**(7), 1339–1362 (1998)
18. Z. Wu, Compactly supported positive definite radial functions. Adv. Comput. Math. **4**(1), 283–292 (1995)
19. H. Wendland, Piecewise polynomial, positive definite and compactly supported radial functions of minimal degree. Adv. Comput. Math. **4**(1), 389–396 (1995)
20. M.D. Buhmann, Radial functions on compact support, in *Proceedings of the Edinburgh Mathematical Society (Series 2)* **41**(01), 33–46 (1998)
21. K.K. Prem, *Fundamental Solutions for Differential Operators and Applications*. (Birkhauser Boston Inc., Cambridge, 1996)
22. A.J. Nowak, A.C. Neves, *The Multiple Reciprocity Boundary Element Method.* (Computational Mechanics Publication, Southampton, 1994)
23. M. Itagaki, Higher order three-dimensional fundamental solutions to the Helmholtz and the modified Helmholtz equations. Eng. Anal. Boundary Elem. **15**, 289–293 (1995)
24. W. Chen, Z.J. Shen, L.J. Shen, G.W. Yuan, General solutions and fundamental solutions of varied orders to the vibrational thin, the Berger, and the Winkler plates. Eng. Anal. Boundary Elem. **29**(7), 699–702 (2005)
25. W. Chen, Meshfree boundary particle method applied to Helmholtz problems. Eng. Anal. Boundary Elem. **26**(7), 577–581 (2002)
26. W. Chen, L.J. Shen, Z.J. Shen, G.W. Yuan, Boundary knot method for Poisson equations. Eng. Anal. Boundary Elem. **29**(8), 756–760 (2005)
27. Y.C. Hon, Z. Wu, A numerical computation for inverse boundary determination problem. Eng. Anal. Boundary Elem. **24**(7–8), 599–606 (2000)
28. E.J. Kansa, Multiquadrics–A scattered data approximation scheme with applications to computational fluid-dynamics–II solutions to parabolic, hyperbolic and elliptic partial differential equations. Comput. Math. Appl. **19**(8–9), 147–161 (1990)
29. Z.J. Fu, W. Chen, A truly boundary-only Meshfree method applied to Kirchhoff plate bending problems. Adv. Appl. Math. Mech. **1**(3), 341–352 (2009)
30. W. Chen, Z.J. Fu, B.T. Jin, A truly boundary-only Meshfree method for inhomogeneous problems based on recursive composite multiple reciprocity technique. Eng. Anal. Boundary Elem. **34**(3), 196–205 (2010)
31. K.E. Atkinson, The numerical evaluation of particular solutions for Poisson's equation. IMA J. Numer. Anal. **5**, 319–338 (1985)
32. C.S. Chen, Y.F. Rashed, Evaluation of thin plate spline based particular solutions for helmholtz-type operators for the drm. Mech. Res. Commun. **25**, 195–201 (1998)

33. A.S. Muleshkov, M.A. Golberg, C.S. Chen, Particular solutions of helmholtz-type operators using higher order polyharmonic splines. Comput. Mech. **24**, 411–419 (1999)
34. A.H.D. Cheng, Particular solutions of Laplacian, helmholtz-type, and polyharmonic operators involving higher order radial basis function. Eng. Anal. Boundary Elem. **24**, 531–538 (2000)
35. A.S. Muleshkov, M.A. Golberg, Particular solutions of the multi-helmholtz-type equation. Eng. Anal. Boundary Elem. **31**, 624–630 (2007)
36. C.S. Chen, Y.C. Hon, R.S. Schaback, *Radial basis function with Scientific Computation* (University of Southern Mississippi, Mississippi, 2007)
37. C.C. Tsai, Particular solutions of splines and monomials for polyharmonic and products of Helmholtz operators. Eng. Anal. Boundary Elem. **33**(4), 514–521 (2009)
38. G.M. Yao, Local Radial Basis Function Methods for Solving Partial Differential Equations. Ph.D. Dissertation, University of Southern Mississippi, 2010
39. R.E. Carlson, T.A. Foley, Interpolation of track data with radial basis methods. Comput. Math. Appl. **24**, 27–34 (1992)
40. Y.C. Shiah, C.L. Tan, BEM treatment of three-dimensional anisotropic field problems by direct domain mapping. Eng. Anal. Boundary Elem. **28**(1), 43–52 (2004)
41. B.T. Jin, W. Chen, Boundary knot method based on geodesic distance for anisotropic problems. J. Comput. Phys. **215**(2), 614–629 (2006)
42. D.E. Myers, S. De Iaco, D. Posa, L. De Cesare, Space-time radial basis function. Comput. Math. Appl. **43**(3–5), 539–549 (2002)
43. W. Chen, New RBF collocation schemes and kernel RBF with applications. Lect. Notes Comput. Sci. Eng. **26**, 75–86 (2002)
44. D.L. Young, C.C. Tsai, K. Murugesan, C.M. Fan, C.W. Chen, Time-dependent fundamental solutions for homogeneous diffusion problems. Eng. Anal. Boundary Elem. **28**(12), 1463–1473 (2004)
45. C.C. Tsai, D.L. Young, C.M. Fan, C.W. Chen, MFS with time-dependent fundamental solutions for unsteady Stokes equations. Eng. Anal. Boundary Elem. **30**(10), 897–908 (2006)
46. W. Chen, M. Tanaka, New Insights into Boundary-only and Domain-type RBF Methods. Int. J. Nonlinear Sci. Numer. Simul. **1**(3), 145–151 (2000)
47. W. Chen, M. Tanaka, Relationship between boundary integral equation and radial basis function. Paper presented at the 52th symposium of Japan society for computational methods in engineering (JASCOME) on BEM, Tokyo
48. W. Chen, M. Tanaka, A meshless, integration-free, and boundary-only RBF technique. Comput. Math. Appl. **43**(3–5), 379–391 (2002)
49. J. Lin, W. Chen, K.Y. Sze, A new radial basis function for Helmholtz problems. Eng. Anal. Boundary Elem. **36**(12), 1923–1930 (2012)
50. S.G. Ahmed, A collocation method using new combined radial basis function of thin plate and multiquadraic types. Eng. Anal. Boundary Elem. **30**(8), 697–701 (2006)
51. B. Fornberg, E. Larsson, G. Wright, A new class of oscillatory radial basis function. Comput. Math. Appl. **51**(8), 1209–1222 (2006)
52. V. Kompis, M. Stiavnicky, M. Zmindak, Z. Murcinkova, Trefftz radial basis function (TRBF), in *Proceedings of Lsame.08: Leuven Symposium on Applied Mechanics in Engineering, Pts 1 and 2*, 25–35 (2008)
53. N.A. Libre, A. Emdadi, E.J. Kansa, M. Shekarchi, M. Rahimian, Wavelet based adaptive RBF method for nearly singular poisson-type problems on irregular domains. CMES Comput. Model. Eng. Sci. **50**(2), 161–190 (2009)